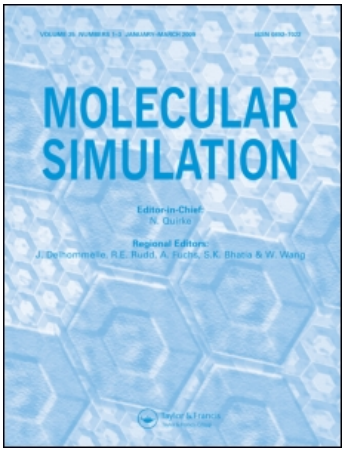

Molecular Simulation

Publication details, including instructions for authors and subscription information:
http://www.informaworld.com/smpp/title~content=t713644482

Modelling of Liquid Crystal Polymers at Different Length Scales

G. Goldbeck-Wood[a]; P. Coulter[a]; J. R. Hobdell[b]; M. S. Lavine[ac]; K. Yonetake[d]; A. H. Windle[a]
[a] Department of Materials Science and Metallurgy, University of Cambridge, Cambridge, UK [b] ICI Polyurethanes, Everberg, Belgium [c] H. H. Wills Physics Laboratory, University of Bristol, Bristol, UK [d] Department of Materials Science and Engineering, Yamagata University, Yamagata, Japan

To cite this Article Goldbeck-Wood, G. , Coulter, P. , Hobdell, J. R. , Lavine, M. S. , Yonetake, K. and Windle, A. H.(1998) 'Modelling of Liquid Crystal Polymers at Different Length Scales', Molecular Simulation, 21: 2, 143 — 160
To link to this Article: DOI: 10.1080/08927029808022056
URL: http://dx.doi.org/10.1080/08927029808022056

Molecular Simulation, 1998, Vol. 21, pp. 143–160
Reprints available directly from the publisher
Photocopying permitted by license only

MODELLING OF LIQUID CRYSTAL POLYMERS AT DIFFERENT LENGTH SCALES

G. GOLDBECK-WOOD[a,*], P. COULTER[a], J. R. HOBDELL[b], M. S. LAVINE[a,**], K. YONETAKE[c] and A. H. WINDLE[a]

[a] *Department of Materials Science and Metallurgy, University of Cambridge, Pembroke Street, Cambridge CB2 3QZ, UK;*
[b] *ICI Polyurethanes, Everslaan 45, Everberg B-3078, Belgium;*
[c] *Department of Materials Science and Engineering, Yamagata University, Jonan-4, Yonezawa, Yamagata, 992, Japan*

(Received November 1997; accepted January 1998)

Structure formation in liquid crystalline polymers involves processes at different length scales. The key stages are the molecular conformations which are the basis of the tendency to form a liquid crystalline phase, and the mesoscale texture of the nematic director field, involving distortion elasticity due to defects. This paper outlines computer modelling at these different length scales as well as an approach towards linking the scales by means of calculating mesoscale model parameters from the molecular modelling. The molecular modelling stage involves the calculation of torsional potentials associated with the backbone of the polymer. These energy functions are required for generating an ensemble of chains from which the persistence length can be determined. The molecular data are used to parameterize the mesoscale modelling: Frank elastic constants, rotational diffusion constant and Ericksen shape parameter are determined. On the mesoscale, a lattice model for the director field is formulated. A Monte Carlo algorithm is employed to study the annealing of the director microstructure. Shearing is added *via* the Ericksen equation and a dynamics model allows simulation of flow of the director field under constant shear. As an example we study the thermotropic aromatic co-polyester Vectra A.

Keywords: Liquid-crystalline polymers; molecular modelling; persistence length; mesoscale modelling; Frank elasticity; Ericksen theory

* Corresponding author.
** Present address: H. H. Wills Physics Laboratory, University of Bristol, Tyndall Avenue, Bristol BS8 1TL, UK.

INTRODUCTION

The work presented here is based on several years of research in the Cambridge group aimed at establishing structure-property relations in an important class of materials, namely the thermotropic liquid-crystalline co-polyesters. These materials were the first synthesised to be liquid-crystalline at sufficiently low temperatures to allow processing in the liquid-crystalline melt [1]. They have found a range of applications related to their low melt viscosity and low shrinkage as well as their strength. Examples are high precision mouldings for electrical connectors and stiff fibres which are the result of highly uniform chain alignment in both the crystalline and the liquid crystalline glass phases.

The final properties of these materials depend upon effects which can be related to different length scales. Liquid crystallinity itself is the result of chain stiffness, hence of largely molecular origin. On the other hand, the strength of the product also depends on defects in the microstructure, *i.e.*, a mesoscale phenomenon.

Therefore we have carried out modelling at the molecular scale as well as on the mesoscale. Single chain conformations and hence stiffness of the material can be deduced from molecular modelling. Mesoscale modelling of the liquid crystal director field provides crucial insight into the defect structure and the interaction of defects with shear is relevant to processing. While both methods provide valuable information in their own right, we have also attempted to connect the length scales by parameterising the mesoscale model on the basis of molecular modelling results. An overview of the modelling hierarchy we employed is shown in Figure 1.

MOLECULAR SYSTEMS

Although the approach presented here is general in nature, and may therefore be applied to a range of different molecular systems, we concentrate on a class of aromatic co-polyesters, known commercially under the tradename Vectra™ [2], and in particular on Vectra A, a random copolymer of 75% hydroxybenzoic acid (HBA) and 25% 6-hydroxy-2-naphthoic acid (HNA). It has a crystal melting point of about 290°C, above which it exhibits a nematic phase.

MOLECULAR MODELLING

The molecular modelling stage serves to gain an understanding of the single chain behaviour at different temperatures, and in particular to determine the

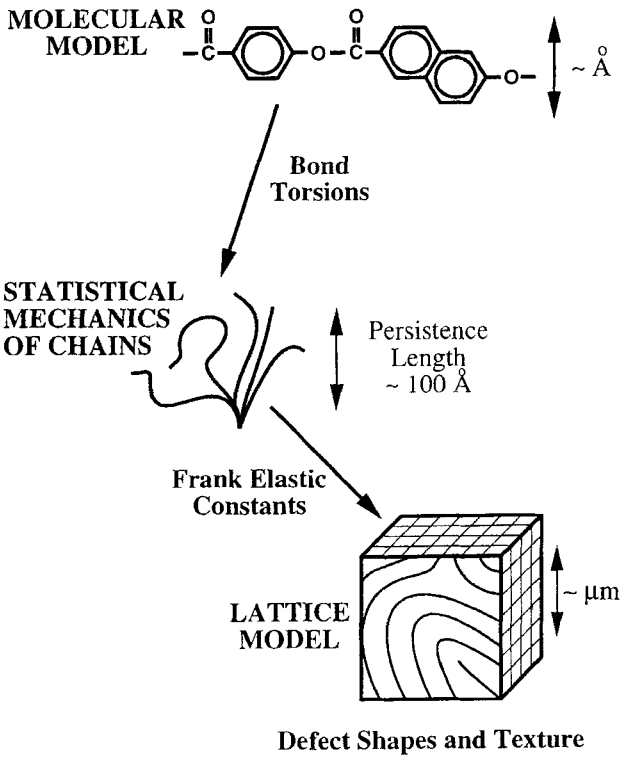

FIGURE 1 Schematic of the modelling hierarchy used in this work, reaching from molecular to mesoscale.

chain persistence length. The latter is defined as the average length of the end-to-end distance of infinite chains projected onto an axis parallel to the 'first' monomer linkage.

In order to obtain realistic values for the persistence length we need to create a statistical ensemble of chain conformations. Although accurate quantum-mechanical calculations can nowadays be made on systems of hundreds of atoms, these are still hardly feasible for chains of say 100 monomers of HBA/HNA. We therefore employ a series of techniques in a hierarchical order starting from the optimised monomer structure, *via* the dimer rotational potentials to the chain properties. As a result we obtain the persistence length, contour length, and diameter of the chains, all of which enter into the parameterization of the mesoscale modelling. These steps are described in more detail in the following sections. For all of our molecular modelling, we use the Cerius and Cerius[2] suites of software from Molecular Simulations Inc. (see also the Special Appendix).

Monomers, Dimers and Rotational Potentials

As a first step we need to generate well optimised monomers. In some cases these are available from libraries, in others such as HNA, we use modelling (*e.g.*, the Cerius[2] Sketcher) to build the monomer and then optimise the structure by a combination of Molecular Mechanics and semi-empirical molecular orbital [3] methods.

In the next step we link pairs of monomers to make all dimers found in the chain. The bonds created in this process will be the rotatable bonds along the backbone of the chain. As an example, Figure 2 shows an aromatic ester moiety which includes the ester link in a similar environment to that found in a chain of Vectra A polymer. Notice the end groups are included in this dimer. The task is now to determine the rotational potentials for the bonds labelled *R*, *S* and *T* in Figure 2. Different methods are at hand to do this. While we generally employ semi-empirical molecular orbital calculations (MOPAC-AM1), we also compare the results with those of force-field based calculations (using Cerius[2] CONFORMATIONAL SEARCH).

The results for the *S* bond of the dimer displayed in Figure 2 are shown in Figure 3. The torsion around this bond has the strongest effect on the 'straightness' of the chain. Firstly, we notice a sharp maximum at 0 deg, which is very large in the case of the force-field calculations. Careful MOPAC calculations (Fig. 3b) confirm that there is a conformational transition, hence a singular point at 0 degrees. This is highlighted by the fact that we find a hysteresis loop as we go past this point in very small torsional steps, as indicated on Figure 3. Secondly, the stiffness of the bond, as given by the curvature of the potential well at 180 degrees, is smaller than that previously reported [4]. Further work using density functional methods is under way to check on this difference.

We furthermore need to consider that because of such delocalization effects, the potential of one rotatable bond may depend on the state of neighbouring or even next-neighbour bonds along the chain. This is of importance in poly(ethylene terephtalate), due to the so-called oxygen-gauche effect [5]. In such a case a series of one-dimensional potential

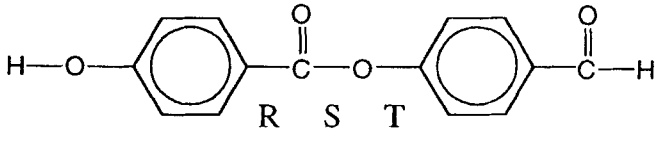

FIGURE 2 Molecular model of a benzoic acid dimer with terminal groups as found in the Vectra A polymer. Also labelled are the rotatable bonds, called *R*, *S* and *T*.

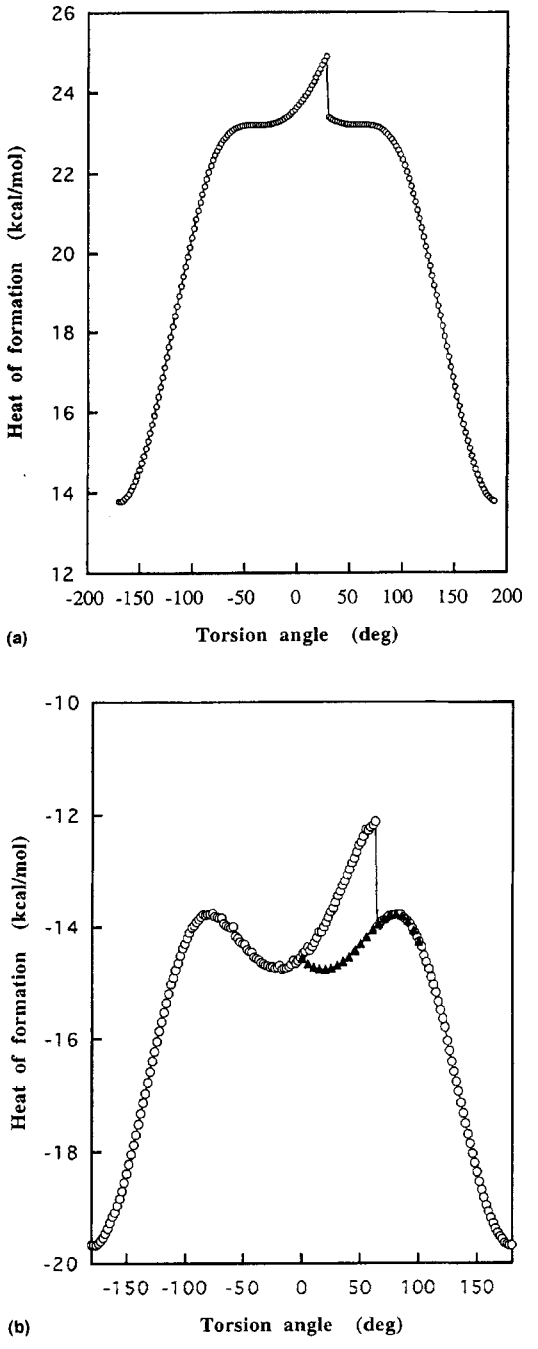

FIGURE 3 Potential of the *S* bond of the dimer shown in Figure 3; (a) as calculated using Conformational Search, and; (b) calculated by MOPAC7-AM1. There is a conformational transition at 0 degrees. As the angle is increased this conformation is retained until a sudden transition takes place, creating a hysteresis loop. Data obtained by decreasing angle are shown as solid triangles.

energies is no longer sufficient to generate a realistic ensemble of chain conformations. Instead, at least two-dimensional energy maps are required.

In the following, however, we shall limit ourselves to the one-dimensional case, having acknowledged its limitations.

Generating an Ensemble of Chain Conformations

The relevant theoretical background is the Rotational Isomeric State theory [6], which basically says that a chain conformation in equilibrium will be determined by a Boltzmann distribution of the dihedral conformations of lowest energy. An extension to this theory is a Monte Carlo algorithm which generates chains by assigning dihedral angles on the basis of complete rotational potential energy functions for each of the bond environments along a chain. Such an algorithm is implemented in the Cerius STATMECH software. By averaging over a large number of chains, single chain properties such as radius of gyration and persistence length can be determined [4]. The results of our simulations of Vectra A using the potentials determined above are in shown Figure 4. The persistence length at 300°C, which lies within the nematic phase, is about 60 Å. This is less than obtained previously [4], which we believe to be largely due to the slightly more flexible *S*-bond potential (see above).

We acknowledge that the single chain persistence length cannot generally be assumed to be a good measure of the behaviour of the chains in bulk melt. Our studies of polymers which do not contain flexible sequences have shown, however, a consistent correlation between the tendency of such polymers to exhibit a nematic phase and the 'aspect' ratio $R_a = q/d$ of the single chain persistence length q and molecular diameter d being greater than five at temperatures where the material is still in the melt [4]. In the light of this evidence we shall henceforth use these single chain quantities as a basis for calculating the elastic constants of Vectra A in the nematic phase.

PARAMETERIZATION

'Parameterization' is the step of linking the length scales by means of condensing the information obtained on a finer scale into parameters used in the simulation on a larger length scale. In the case in hand the key parameters determining the microstructure in a quiescent nematic phase are firstly the nematic director itself, representing the orientation of many

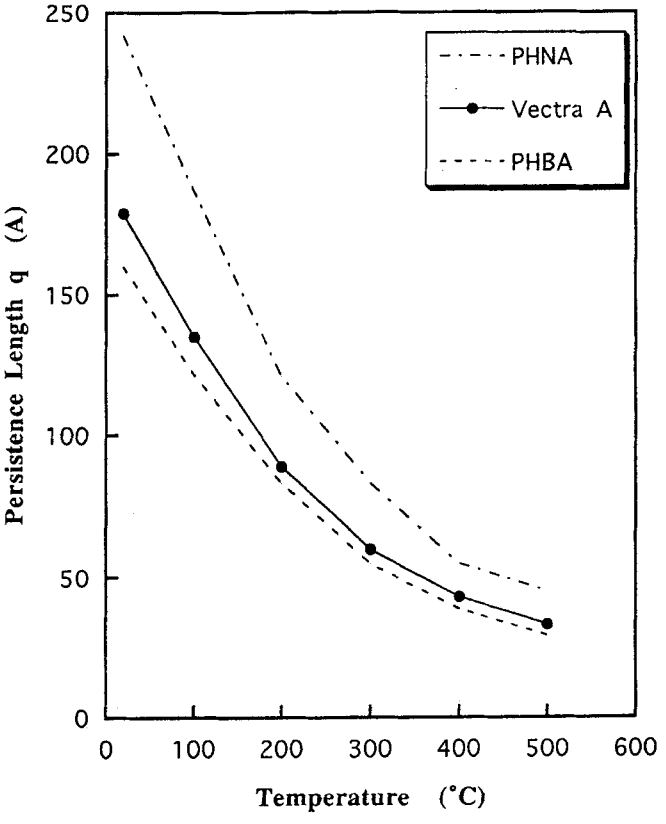

FIGURE 4 Persistence lengths of Vectra A copolymer, as well as HBA and HNA homopolymers. The degree of polymerization is 200.

molecules, and secondly the three Frank elastic constants. As we add an external shear field, two additional parameters come into play. Firstly, the so-called shear response parameter λ, and secondly the rotational viscosity ζ_r.

The Nematic Director

The director $\boldsymbol{n}$ of a nematic liquid crystal is related to the probability density of molecular orientations $\boldsymbol{u}$ in a region of space *via* the molecular anisotropy tensor $\boldsymbol{S}$:

$$S_{\alpha\beta} = V_{\text{cell}}^{-1} \int_{\text{cell}} \left\langle u_\alpha u_\beta - \frac{1}{3} \delta_{\alpha\beta} \right\rangle \tag{1}$$

where the integral extends over one lattice cell of volume V_{cell} (Fig. 5). In the unixial nematic phase $\boldsymbol{S}$ has only one eigenvector, which is the director $\boldsymbol{n}(x, t)$, with an eigenvalue proportional to the scalar order parameter P_2. In a sample containing defects the largest cell volume V_{cell} we can choose is determined by the radius of a defect core. In the Vectra A materials this is about 10^{-7} m. The degree of orientation within each cell, P_2, is then assumed to be constant for a sample deep inside the nematic phase.

The Frank Elastic Constants

As we consider the material to be well within the liquid crystalline phase, the lowest free energy state is reached if all the molecules are aligned. Any deviations from this state raise the energy. Frank formulated a theory of distortions which takes into account the symmetries of the phase [7]. As a result of nematic symmetry, three different distortions arise, known as 'splay', 'twist' and 'bend', as indicated in Figure 6. Associated with each type of distortion is an elastic energy, which is a material constant. In the case of polymer liquid crystals it is of particular importance to distinguish between the contributions of splay, twist and bend distortions, as a brief inspection of Figure 6 will indicate. Consider the rods to represent sections of the polymer chain of the size of a persistence length. The first thing to notice is that the twist energy should depend only weakly on this length. Bending, on the other hand will become more and more difficult the longer the units are whereas splay depends most strongly on the length. In fact the lack of chain ends in polymers to fill the gaps makes this parameter depend

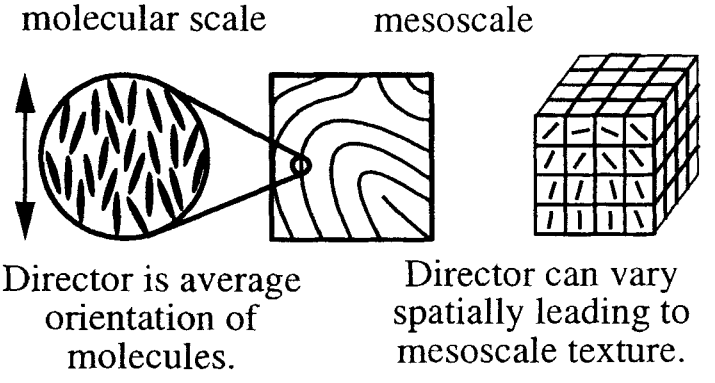

FIGURE 5 Schematic of a liquid crystalline director defining the average orientation of rod-like molecules. Each cell in the lattice model shown represents a director. The size scale of a cell is dictated by the distortions, and is about 10^{-7}m.

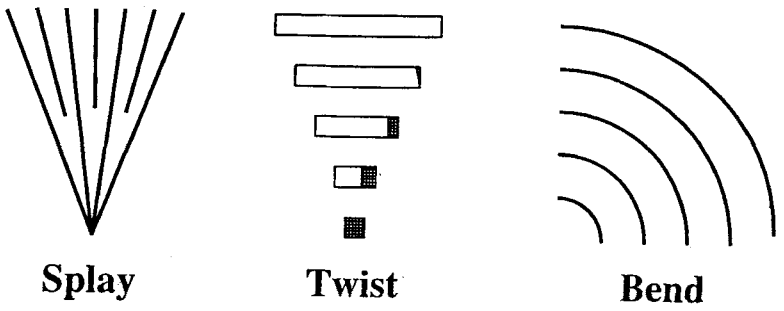

FIGURE 6 Illustration of splay, twist and bend distortions of a nematic phase.

on the contour length L. The equations relating the Frank constants to the molecular quantities have been derived by Odijk [8] and Meyer [9]:

$$\begin{aligned} k_1 &\approx (7/8\pi)(kT/d)\Phi(L/d) \\ k_2 &\approx (kT/d)\Phi^{1/3}R_a^{1/3} \\ k_3 &\approx (kT/d)\Phi R_a \end{aligned} \tag{2}$$

Here L is the contour length, R_a the ratio of persistence length q and diameter d of the chain, Φ is the volume fraction (which is taken as one for a thermotropic polymer), k is the Boltzmann constant and T is the temperature. For a Vectra A type copolyester of molecular weight 20 000 g/mol, using the molecular data determined above for $T = 600\,\text{K}$ ($d = 5\,\text{Å}$, $q = 60\,\text{Å}$, $L = 1000\,\text{Å}$) one obtains the following values: $k_1 \approx 10^{-9}\,\text{N}$, $k_2 \approx 3 \times 10^{-11}\,\text{N}$, $k_3 \approx 2 \times 10^{-10}\,\text{N}$.

Experimental measurement of the elastic constants of liquid crystal polymers are very difficult, and very few reliable data exist. For a co-polyesteramide of similar molecular weight from the Vectra series de'Nève *et al.* [10] found values in the same size order as those above but larger in absolute value by a factor of ten. Further theoretical and experimental work is required to account for this apparent discrepancy.

The Shear Response Parameter

As we add an external shear field to the simulations, knowledge of the relative response of the director to the rotational and extensional components of the shear field is required. In rheology, a factor λ is used to describe the ratio of the extensional to the rotational components of the director flow response [11]. Hence if $\lambda < 1$, the rotational component dominates, leading to a tumbling of the director, whereas for $\lambda > 1$ the

extensional component dominates leading to a stable orientation in the flow field. The case of $\lambda = 1$ is equivalent to that of an affine deformation of the director field.

On a molecular scale λ can be related to the aspect ratio of rigid rods in the simulation. The validity of such an approach in the case of semi-flexible polymers is of course questionable, since other effects such as some sort of entanglement or 'ravelling' may come into play. Nevertheless, for lack of a better expression we shall base our parametrization on such a quasi-molecular picture, and define the 'shear response' parameter as

$$\lambda = (R_a^2 - 1)/(R_a^2 + 1) \tag{3}$$

where R_a is the ratio of persistence length over diameter as defined above. Given the values of q and d we determined for Vectra A, λ will be close to unity, hence the tumbling tendency should be weak. This is in line with the experimental observations of very high local order in these materials [12–14].

The Rotational Viscosity

As with the shear response parameter, there is no adequate expression for the rotational viscosity of thermotropic liquid crystalline polymers. We therefore use an expression for the rotational friction constant of rigid rods [15], substituting the rod length by the persistence length of the polymer

$$\zeta_r = v \frac{\pi \eta q^3}{4} \tag{4}$$

where η is now the 'effective' viscosity of the medium felt by each polymer section of length q, and the concentration v of 'rods' is related to the volume fraction by

$$v = \frac{4\Phi}{\pi d^2 q} \tag{5}$$

Hence in the case of thermotropic liquid crystal polymers ($\Phi = 1$), we obtain a relationship of the form

$$\zeta_r = \beta \eta R_a^2 \tag{6}$$

with some constant β, which empirically is of the order 10^{-4} [16]. Using a typical viscosity of the Vectra material of 10^3 Pa · s, and the data for R_a as

above yields a rotational viscosity of about 10 Pa · s, which is the value used in the simulations below.

A second approach is based on the measurements of viscoelastic coefficients for a lyotropic system (PBG) [17] which indicates that the rotational viscosity in fact scales with the chain length as:

$$\zeta_r = \beta' \eta_{\text{bend}} (L/d)^2 \tag{7}$$

where the bend viscosity η_{bend} is a constant for chain lengths larger than the persistence length. Further work is clearly required to determine satisfactory relationships between molecular parameters and mesoscale modelling parameters.

MESOSCALE MODELLING

Taking a big step up in length scale we now consider the microstructure of a nematic liquid crystalline bulk. The variation of the director orientation within a sample yields a structure map. In the model considered here, this field is represented by a cubic lattice.

Monte Carlo Modelling of Microstructure

Under quiescent conditions, without any external fields applied, the nematic director microstructure will evolve towards its lowest free energy state. We have modelled this annealing process on the basis of the Frank expression for the distortion free energy [7]:

$$U_d = 0.5 * [k_1(\nabla \cdot \boldsymbol{n})^2 + k_2(\boldsymbol{n} \cdot \nabla \wedge \boldsymbol{n})^2 + k_3(\boldsymbol{n} \wedge \nabla \wedge \boldsymbol{n})^2] \tag{8}$$

While a simplified version of this free energy equation, with only a single elastic constant, is often used, clearly the results for the constants obtained in the last section suggest that the full expression with three constants must be used to describe polymer liquid crystals adequately.

The details of the model have been described elsewhere [18]. In outline, an interaction energy for a director with each of its six nearest neighbours is calculated by discretizing the Frank equation (8). Care must be taken to represent the correct symmetry of the system, namely that $\boldsymbol{n}$ is equivalent to $-\boldsymbol{n}$. Furthermore, in the discretization of the derivatives, forward differences must be used to ensure a dependency on the orientation of the

central cell. To retain symmetry, averages are taken after squaring of the contributions calculated on the basis of all eight neighbours. The annealing of the system is then simulated by a Metropolis Monte Carlo algorithm.

To complete the definition of the model, initial as well as boundary conditions must be set. Since we are here interested in the behaviour of the bulk, we employ periodic boundary conditions. As a starting point we choose a random director field.

The Metropolis annealing process takes the structure towards a mono-domain. Observing the intermediate states, we notice the similarity with the experimentally observed microstructure. In particular, as shown in Figure 7a swirling defect is found typically in the simulations using the ratio of Frank constants as determined for the Vectra A material. The similarity with the texture of the fracture surface of this material is remarkable. Only by introducing the different elastic constants in the way given by the Frank equation, have we been able to reproduce this experimental observation on polymeric liquid crystals. For further results of the Monte Carlo simulation such as simulating the Freedericks transitions, we refer to [18].

Dynamics Modelling of Shearing

It is known from experiments that the response of a nematic fluid to an applied shear flow field is complex and very rich in textures. Apart from this scientific interest, there is strong industrial interest in understanding the behaviour of liquid crystalline polymers in processing conditions such as extrusion and injection moulding, which often generate strong shear fields.

The theories most widely used to describe the flow behaviour of liquid crystals are those by Ericksen/Leslie [19] and Doi [15]. The former is based on constitutive equations and provides an equation for a homogeneous director field $\boldsymbol{n}$ subject to an applied flow. The latter is based on a 'molecular' description of rigid rods. Both theories are linear response treatments to the velocity gradient field, expressed by the tensor

$$K_{ij} = \partial_i \nu_j, \tag{9}$$

where i, j denote the three Cartesian co-ordinates.

Despite the different derivations, the Doi equation for the response of the rigid rod to an external flow and the Ericksen equation for the director response are actually mathematically identical. The Ericksen equation for

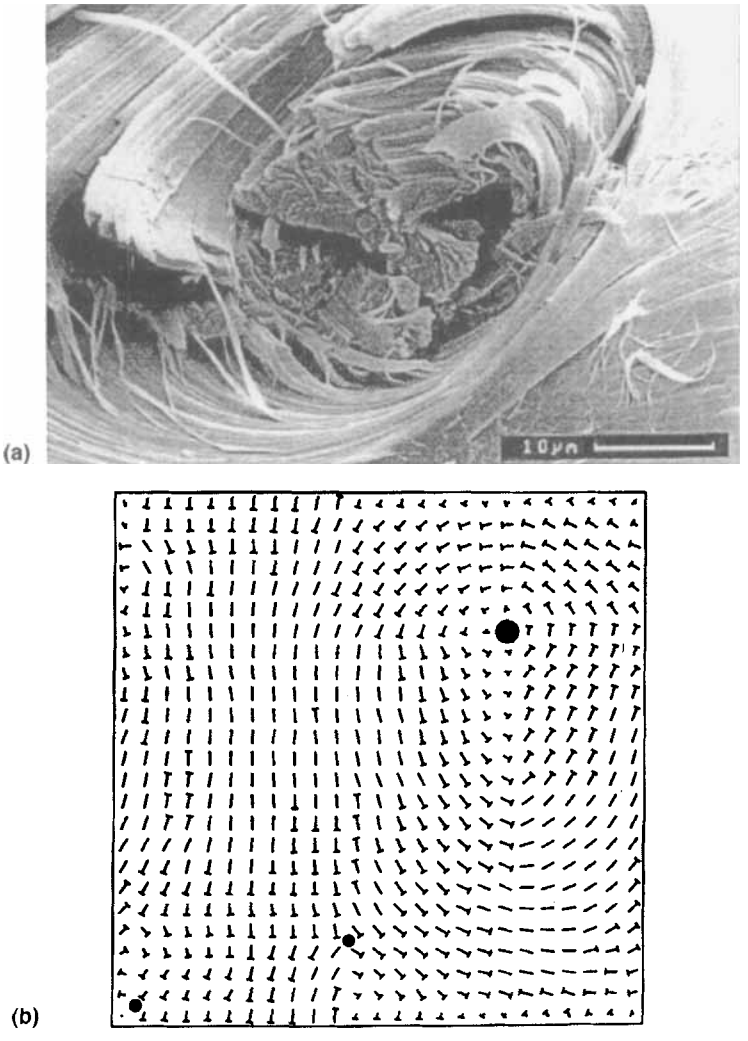

FIGURE 7 Experimentally observed microstructure and simulated director field. (a) A fracture surface of Vectra A of molecular mass 5000 g mol^{-1}, quenched from the nematic melt. The fibres seen are parallel to the molecular axis. (b) Part of a section through a Monte Carlo annealing simulation run on an 48^3 lattice with periodic boundary conditions. The elastic constants were chosen to have a splay:twist:bend ratio of 300:1:30. The directors are represented by nails with the length of the shaft being proportional to the in-plane component of the director and the points pointing out of the plane. Note the swirling pattern which resembles the experimentally observed feature. Such swirls are characteristic of simulations in which the splay elastic constant is high and the twist constant is low, and are not seen in other simulations.

the rate of change of a director $\boldsymbol{n}$ subject to an applied flow field is usually written in the following way:

$$\dot{\boldsymbol{n}} = \boldsymbol{n} \cdot \omega + \lambda(\boldsymbol{n} \cdot \boldsymbol{A} - \boldsymbol{A} : \boldsymbol{nnn}) \tag{10}$$

where $\boldsymbol{A}$ is the symmetric part of the velocity gradient tensor (6), also known as the strain rate tensor, ω is the antisymmetric part of $\boldsymbol{K}$, known as the vorticity tensor, and λ is the molecular shape parameter already defined above.

The Doi theory, on the other hand, yields the expression for the orientation of the rigid rod molecule, described by its axial vector $\boldsymbol{u}$ as

$$\dot{\boldsymbol{u}} = \boldsymbol{u} \cdot \boldsymbol{K} - \boldsymbol{K} : \boldsymbol{uuu} \tag{11}$$

It is straightforward to see that both equations are actually mathematically identical in the case of $\lambda = 1$.

Both Ericksen and Doi developed their theories for initially uniform orientation. Although extensions of these theories include polydomain effects, they are still not able to provide detailed information about microstructural evolution and interactions between flow and defects. Therefore we have developed the mesoscale lattice model further so as to combine shear flow and distortion elasticity responses on a local scale.

We start off with the Ericksen equation, and then add the response due to distortion elasticity. This yields a dynamic equation for each individual director in a mean-field of distortion elasticity and shear flow.

$$\dot{\boldsymbol{n}} = \boldsymbol{n} \cdot \omega + \lambda(\boldsymbol{n} \cdot \boldsymbol{A} - \boldsymbol{A} : \boldsymbol{nnn}) + \zeta_r^{-1} \delta U_d / \delta \boldsymbol{n} \tag{12}$$

On this basis we carry out simulations by updating the whole lattice in each iteration, according to the following three calculations:

- the net rotation of the director as a response to the applied shear field.
- the macroscopic translation of the fluid element as a result of the flow field.
- the net distortion force as resulting from the Frank elasticity.

Although this approach can in principle be followed through for the complete Frank equation, we restrict ourselves here to a simpler expression, approximating the distortion energy by:

$$U_d = \frac{k}{2} \sum_i \sin^2(\Delta\theta_i) \tag{13}$$

where the single Frank constant is $k = k_1 = k_2 = k_3$, $\Delta\theta_i$ is the angle between the central director and a neighbouring director, and the summation is over nearest neighbours. Details of this choice and its advantages have been discussed elsewhere [20].

We have carried out simulations for a range of conditions, in both two and three dimensions. Investigating the response of a single disclination loop to the director field we find that there is a strong dependency on the 'rotation vector' of a 'Class I' loop, *i.e.*, the details of its director distortion geometry. In one extreme, the loop will self-annihilate, as in the quiescent state, while in the other the flow elongates the loop and actually prevents its collapse. Details are discussed in a separate paper [21].

We present here further results of some two dimensional simulations. Typical microstructures of simulations with homeotropic boundary conditions are shown in Figure 8. We note that at low shear rates the effect of the fixed boundary orientation permeates throughout the thickness of the sample. At medium shear rates, the boundary aligned regions still cover an area similar in size to that of the flow aligned region. As the shear rate is increased further, the boundary region is reduced to just a few layers. The flow aligned region, on the other hand, does not simply get bigger. Distortions lead to the formation of some vorticity aligned layers which alternate with flow aligned layers. We have also seen this tendency to form layers in our three-dimensional simulations, which will be published elsewhere.

We have calculated the stresses which result from the viscous flow and the distortion elasticity present in the simulations, in analogy to the derivation in the case of rigid rods [15]. For the viscous stress, assuming rotational frictional work done for each molecule contained within a director cell we find:

$$\sigma_{vis} = DA\langle n_k n_l n_i n_j \rangle \tag{14}$$

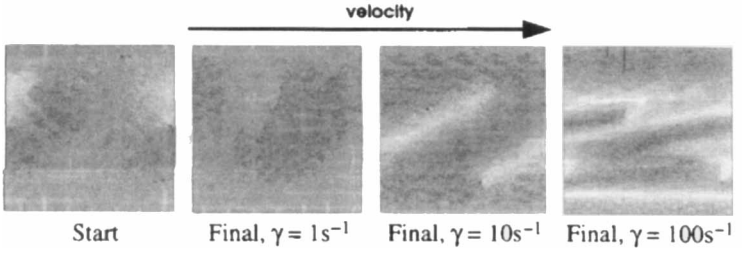

FIGURE 8 Director microstructures obtained by shearing at different rates as indicated. Colour coding is used to show the orientation with blue for velocity alignment, green for velocity gradient alignment, and red for vorticity (out-of-plane) alignment. The lattice size is 100*100, with homeotropic boundary conditions at the top and bottom.

The elastic response has two terms on the molecular scale, one related to the molecular entropy (proportional to kT), the other to the coupling of the molecules with the elastic torque τ. Since the directors in our description average over a volume of $(100\,\text{nm})^3$, the entropic term becomes negligible, and we are left with the coupling of the elastic torque τ and the director field, given by:

$$\sigma_{\text{elastic}} = k\langle(n \times \tau)_i n_j\rangle \tag{15}$$

Here the elastic torque τ is given by the derivative of the distortion energy with angle

$$\tau = k \sum_i \sin(\Delta\theta_i)\cos(\Delta\theta_i)|\boldsymbol{n} \times \boldsymbol{n}_i| \tag{16}$$

The 'steady-state' viscosities at constant strain, given by stress over shear rate, for the range of two-dimensional simulations are shown in Figure 9. We notice the typical shear thinning behaviour. The elastic component decreases approximately linearly in this log–log plot, in fact $\sigma_{\text{elastic}} \approx \dot{\gamma}^{1/2}$, whereas the viscous component is independent of shear rate up to about $10\,\text{s}^{-1}$, and then shows a sharp break to follow along a similar 1/2 gradient to the elastic part. The low shear rate behaviour is hence similar to that determined by Marrucci for the shear-thinning Region I of liquid crystal polymers [22].

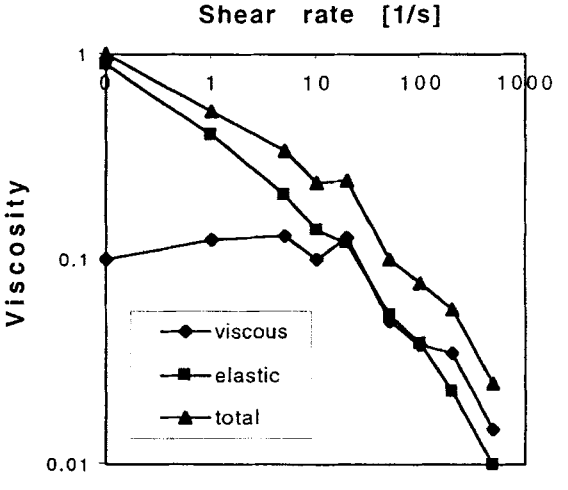

FIGURE 9 Steady state viscosities obtained from the imposed shear simulations, showing shear thinning behaviour.

CONCLUSIONS AND FURTHER WORK

We have followed a hierarchical modelling route to investigate structure formation in liquid crystalline co-polyesters. These materials, despite their complexities and richness of structure, have nevertheless proven to be excellent candidates for the hierarchical approach. The reasons for this are (1) the fact that single chain modelling can furnish a quantity (persistence length) which is a key input parameter to the mesoscale modelling, and (2) mesoscale modelling of the structure provides a good approximation to the structure of the solidified product since the changes on crystallization of these materials are small, unlike in flexible semi-crystalline polymers. We are hoping to build further on this scheme by (1) improving the single chain conformations by means of using more ab initio calculations, as well as two-dimensional rotational potentials, (2) introducing separate elastic constants for splay, twist and bend into the flow modelling, and (3) by linking the mesoscale models with macromodels including the filling of injection moulding parts, heat flow and solidification.

Acknowledgements

We would like to acknowledge financial support for this work by EPSRC and Hoechst Celanese, and we would like to thank Molecular Simulations Inc. for providing the software.

SPECIAL APPENDIX

For molecular simulations in this paper the following modules and settings of the Cerius[2] software from Molecular Simulations Inc have been used:

- Sketcher and Polymer Builder to build monomers and dimers
- Force field: pcff 300
- Conformational Search: Grid Scan with 'Minimize Conformation' switched on
- MOPAC6 and MOPAC7–AM1: Scan Potential Surface–one dimensional.

References

[1] Jackson, W. J. and Kuhfuss, H. F. (1976). *J. Polym. Sci. Poly. Chem.*, **14**, 2043.
[2] Vectra, a registered tradename by Hoechst Celanese Corp., Summit, NJ, 1985.

[3] Stewart, J. J. P. (1987). MOPAC, QCPE, Frank J., Seiler Research Laboratory, USAF Academy, Colorado Springs, CO.
[4] Bedford, S. E., Yu, K. and Windle, A. H. (1992). "Influence of chain flexibility on polymer mesogenicity", *J. Chem. Soc. Faraday Trans.*, **88**, 1765.
[5] Smith, G. D., Yoon, D. Y. and Jaffe, R. L. (1993). "A 3rd-order rotational isomeric state model for poly(oxyethylene) based upon *ab-initio* electronic-structure analyses of model molecules", *Macromolecules*, **19**, 5213 .
[6] Flory, P. J. (1969). "Statistical mechanics of chain molecules", Wiley (Interscience), New York.
[7] Frank, F. C. (1958). "On the theory of liquid crystals", *Discuss. Faraday Soc.*, **25**, 19.
[8] Odijk, T. (1986). *Liquid Crystals*, **7**, 553.
[9] Meyer, R. B. (1982). In: *Polymer Liquid Crystals*, Krigbaum, W. R., Ciferri, A. and Meyer, R. B., Eds., Academic Press, New York, 1982, pp. 133–164.
[10] De'Nève, T., Kléman, M. and Navard, P. (1995). "Observation of textures of nematic polymers and estimation of the elastic-constants", *Liquid Crystals*, **18**, 67.
[11] Ericksen, J. L. (1960). *Arch. Ration. Mech. Anal.*, **4**, 231 and *Kolloid-Z*, **173**, 117.
[12] Mitchell, G. R. and Windle, A. H. (1983). *Polymer*, **24**, 1513.
[13] Li, M. H., Brulet, A., Cotton, J. P., Davidson, P., Strazielle, C. and Keller, P. (1994). *J. Phys. (Paris)*, **4**, 1843.
[14] Dreher, S., Zachmann, H. G., Riekel, C. and Engstrom, P. (1995). *Macromols.*, **28**, 7071.
[15] Doi, M. and Edwards, S. F. (1986). "The theory of polymer dynamics", Clarendon Press, Oxford.
[16] Larson, R. G. (1996). "On the relative magnitudes of viscous, elastic and texture stresses in liquid crystalline PBG solutions", *Rheol. Acta*, **35**, 150.
[17] Lee, S.-D. and Meyer, R. B. (1990). "Light scattering measurements of the anisotropic viscoelastic coefficients of a main-chain polymer nematic liquid crystal", *Liquid Crystals*, **7**, 15.
[18] Hobdell, J. R. and Windle, A. H. (1997). "A numerical technique for predicting microstructure in liquid crystalline polymers", *Liquid Crystals*, **23**, 157.
[19] Leslie, F. M. (1966). *Q. J. Mech. Appl. Math.*, **XIX**, 357.
[20] Lavine, M. S. (1996). *Ph.D. Thesis*, University of Cambridge.
[21] Lavine, M. S. and Windle, A. H. (1997). "Computational modelling of disclination loops under shear flow", *Macromol. Symp.*, **124**, 35.
[22] Marrucci, G. (1991). "Tumbling regime of liquid-crystalline polymers", *Macromolecules*, **24**, 4176.